Published in final edited form as:
J Am Chem Soc. 2007 February 14; 129(6): 1769–1775.

Symmetry control of radiative decay in linear polyenes: Low barriers for isomerization in the S_1 state of hexadecaheptaene

Ronald L. Christensen[1], **Mary Grace I. Galinato**[2], **Emily F. Chu**[2], **Ritsuko Fujii**[3], **Hideki Hashimoto**[4], and **Harry A. Frank**[2]

1 *Department of Chemistry, Bowdoin College, Brunswick, ME 04011-8466, USA*

2 *Department of Chemistry, 55 North Eagleville Road, University of Connecticut, Storrs, CT 06269-3060, USA*

3 *Department of Physics, Osaka City University, 3-3-138 Sugimoto, Sumiyoshi-ku, Osaka 558-8585, Japan*

4 *"Light and Control" PRESTO/JST, 4-1-8 Honcho Kawaguchi, Saitama 332-0012, Japan*

Abstract

The room temperature absorption and emission spectra of the 4-*cis* and *all-trans* isomers of 2,4,6,8,10,12,14-hexadecaheptaene are almost identical, exhibiting the characteristic dual emissions $S_1 \rightarrow S_0$ ($2^1A_g^- \rightarrow 1^1A_g^-$) and $S_2 \rightarrow S_0$ ($1^1B_u^+ \rightarrow 1^1A_g^-$) noted in previous studies of intermediate length polyenes and carotenoids. The ratio of the $S_1 \rightarrow S_0$ and $S_2 \rightarrow S_0$ emission yields for the *cis* isomer increases by a factor of ~15 upon cooling to 77 K in *n*-pentadecane. In contrast, for the *trans* isomer this ratio shows a two-fold decrease with decreasing temperature. These results suggest a low barrier for conversion between the 4-*cis* and *all-trans* isomers in the S_1 state. At 77 K, the *cis* isomer cannot convert to the more stable *all-trans* isomer in the $2^1A_g^-$ state, resulting in the striking increase in its $S_1 \rightarrow S_0$ fluorescence. These experiments imply that the S_1 states of longer polyenes have local energy minima, corresponding to a range of conformations and isomers, separated by relatively low (2–4 kcal) barriers. Steady state and time-resolved optical measurements on the S_1 states in solution thus may sample a distribution of conformers and geometric isomers, even for samples represented by a single, dominant ground state structure. Complex S_1 potential energy surfaces may help explain the complicated $S_2 \rightarrow S_1$ relaxation kinetics of many carotenoids. The finding that fluorescence from linear polyenes is so strongly dependent on molecular symmetry requires a reevaluation of the literature on the radiative properties of *all-trans* polyenes and carotenoids.

INTRODUCTION

The optical spectroscopy of short, *all-trans* polyenes reveals an excited $2^1A_g^-$ singlet state, into which absorption is forbidden by symmetry, lying at lower energy than the $1^1B_u^+$ state responsible for the characteristic strong visible absorption (S_0 ($1^1A_g^-$) → S_2 ($1^1B_u^+$)) in these C_{2h} symmetric, linearly-conjugated π-electron systems.[1,2] This explains several distinctive aspects of polyene optical spectroscopy, including the systematic differences in the transition energies of the strong absorption and the fluorescence (S_1 ($2^1A_g^-$) → S_0 ($1^1A_g^-$)), the anomalously long radiative lifetimes, and the relative insensitivity of the fluorescence spectra to solvent polarizability.[2] Theoretical analysis by Schulten and Karplus[3] of short, *all-trans* polyenes rationalized the low lying S_1 ($2^1A_g^-$) state in terms of extensive configuration interaction between singly and multiply excited singlet configurations with the same symmetry.

Email: rchriste@bowdoin.edu; harry.frank@uconn.edu.

Extensions of this model to longer polyenes and carotenoids predict additional low-lying $^1A_g^-$ and $^1B_u^-$ excited states[4,5], but these other states are not easily detected, either in conventional steady-state or time-resolved spectroscopic measurements.

The theoretical descriptions of *all-trans* polyene excited states have had considerable influence, not only in interpreting the spectroscopy and photophysics of *all-trans* polyenes, but also in explaining optical measurements on a variety of less symmetric polyenes and carotenoids. For example, Koyama, et al.[6,7] assigned features in resonance Raman excitation profiles and in the fluorescence spectra of long carotenoids to low-lying $1^1B_u^-$ states. This group also used ultrafast optical spectroscopy to detect transient absorption features, again attributed to the $1^1B_u^-$ state.[8,9] Cerullo et al.[10] presented ultrafast spectroscopic evidence for an intermediate singlet state (S_x) in several carotenoids, which they postulated facilitates internal conversion between the S_2 ($1^1B_u^+$) and S_1 ($2^1A_g^-$) states. Van Grondelle and coworkers[11] observed a wavelength dependence of the dynamics of spirilloxanthin that was interpreted in terms of another singlet electronic state, S*, thought to be an intermediate in the depopulation of S_2 ($1^1B_u^+$). Fast pump–probe optical techniques were applied to β-carotene by Larsen, et al.[12], and the results suggested yet another carotenoid excited state ($S^‡$) formed directly from S_2 ($1^1B_u^+$). The nature of these states remains uncertain, and recent work has called into question the assignments and suggested that at least some of the spectroscopic observations may be attributed to two-photon processes rather than additional electronic states.[13,14]

Advances in synthetic procedures coupled with improved purification and analytical techniques (HPLC, MS/APCI+, and NMR) have allowed us to revisit the electronic states of simple *all-trans* dimethyl polyenes and to extend optical experiments to their less symmetric *cis* counterparts. These studies reveal that the rates of radiative decay from the "S_1 ($2^1A_g^-$)" states of *cis* polyenes are significantly larger than radiative decay rates from the S_1 ($2^1A_g^-$) states of *trans* polyenes. Our experiments also suggest that *trans* ↔ *cis* conversion readily occurs on the S_1 ($2^1A_g^-$) potential surface. The photochemical formation of *cis* isomers from *trans* ground states requires a reevaluation of previous reports of fluorescence from *trans* polyenes and carotenoids. Many of these studies were carried out prior to the advent of sophisticated high performance liquid chromatography (HPLC) techniques capable of achieving the high level of sample purity and analysis[2,15–27] required to identify the source of fluorescence signals. The work presented here provides an alternate model for internal conversion following the excitation of S_2 ($1^1B_u^+$) and suggests that at least some of the electronic states postulated in recent years may be associated with different geometric isomers and/or conformers formed in the S_1 ($2^1A_g^-$) state. Many of the essential features of the simple "three state" scheme, E (S_2 ($1^1B_u^+$)) > E (S_1 ($2^1A_g^-$)) > E (S_0 ($1^1A_g^-$)), are preserved by invoking isomerization and/or conformational change on short time scales in the S_1 ($2^1A_g^-$) state.

EXPERIMENTAL

2,4,6,8,10,12,14-hexadecaheptaene was synthesized via a Wittig reaction between 2,4,6,8,10,12-dodecapentaenal and crotyltriphenylphosphonium bromide. The hexadecaheptaene products were isolated using silica gel chromatography and then photolyzed to convert the predominantly *cis* mixture into the *all-trans* isomer. HPLC (C_{18}- reverse phase) was used to isolate the *cis* and *trans* isomers for spectroscopic analysis. Mass spectrometry (MS/APCI+) and NMR spectroscopy (2D ^1H-^1H COSY and NOESY) were used to identify the major product of the Wittig reaction as 4-*cis* hexadecaheptaene. The main photolysis product is the *all-trans* isomer, as summarized in the following reaction scheme:

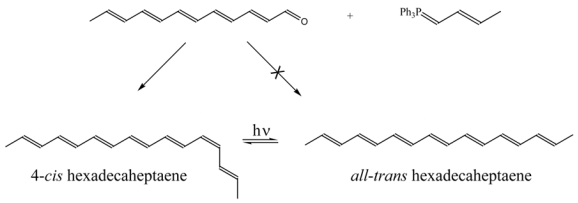

Synthesis of 4-*cis* hexadecaheptaene

All-trans 2,4,6,8,10,12-dodecapentaenal was obtained by condensing crotonaldehyde (Sigma-Aldrich) as described previously.[19,28,29] 50 mg of the crotyl ylide (Fluka) was combined with 1 mL of anhydrous THF in a 5-mL flask. 17 mg of the dodecapentaenal was added and the mixture stirred for 30 minutes. The characteristic polyene absorption (300–400 nm) was used to follow the buildup of the heptaene product. Aqueous NaOH was added to quench the reaction and the hexadecaheptaene extracted using several aliquots of warm hexane. The crude hexadecaheptaene was purified on silica gel (Silica Gel 60 -EM Reagents) using hexane as a mobile phase.

Photoisomerization and high-performance liquid chromatography (HPLC) of hexadecaheptaene

Hexadecaheptaene fractions collected from the silica gel column were evaporated and re-constituted in acetonitrile (Fisher Scientific, HPLC-grade) and placed in a 1-cm path length quartz spectrophotometer cell. The sample (Absorbance ~1.6) was exposed to 396 nm light with a 14.7 nm bandpass using a Jobin-Yvon Horiba Fluorolog-3 fluorescence spectrometer (see below). The illumination was interrupted every 5 minutes to mix the sample and to record the absorption spectrum. The total sample illumination time was 30 minutes. The photolyzed sample was analyzed using a Waters HPLC equipped with a 600S controller, a 616 pump and a 717plus autosampler. A Waters 996 photodiode array detector (PDA) monitored the absorption spectra of the peaks as they eluted from a Nova-Pak reverse-phase C18 column (3.9 × 300 mm, 60 Å pore size and 4 μm particle size of spherical amorphous silica). Acetonitrile was used as the mobile phase, and the system was run in isocratic mode at a flow rate of 0.5 mL/min.

Characterization of hexadecaheptaene isomers by nuclear magnetic resonance spectroscopy

The dominant isomer in the unphotolyzed hexadecaheptaene sample (Fig. 1) was isolated by HPLC using a 250 × 4.6 mm YMC-Pak C_{18}-A column (5-μm particle size, 12-nm pore size) and acetonitrile as the mobile phase. 1D and 2D ^{1}H NMR spectra, including ^{1}H-^{1}H COSY and ^{1}H-^{1}H NOESY spectra, were recorded in chloroform-D at room temperature using a 600 MHz FT NMR spectrometer. Proton signals corresponding to the methyl groups showed distinct chemical shifts, indicating an asymmetric structure. Exploiting the 2D correlation peaks starting from the methyl protons, signals due to the ethylenic protons were assigned based on splittings, coupling constants, and COSY cross peaks between neighboring protons. These assignments are summarized in Figure S1 (Supporting Information). NOE correlations also proved useful in determining the isomeric configuration, e.g., the clear NOE correlation between 3H and 6H confirmed that the 4C=5C bond had a *cis* configuration. Other NOE correlations confirmed *trans* geometries for the other double bonds. The isomer thus was assigned unequivocally as 4-*cis* hexadecaheptaene.

Fluorescence spectroscopy

Individual HPLC peaks were collected, evaporated, and reconstituted in *n*-pentadecane for fluorescence and fluorescence excitation measurements. Samples were reinjected into the

HPLC after spectroscopic experiments to verify their isomeric purity after exposure to light. Fluorescence spectra were acquired using a Jobin-Yvon Horiba Fluorolog-3 Model FL3-22 spectrometer equipped with double monochromators with 1200 grooves/mm gratings, a Hamamatsu R928P photomultiplier, and a 450 W OSRAM XBO xenon arc lamp. The emission was monitored using front-face detection for the low temperature experiments and right-angle detection for the room temperature measurements. A home-built, flowing gaseous N_2 quartz cryostat maintained sample temperatures between 77 and 300 K. A gold-chromel thermocouple connected to an Air Products digital temperature controller monitored sample temperatures. For studies of the temperature dependence of fluorescence, purified samples were quickly frozen in liquid nitrogen and then transferred to the flowing N_2 cryostat. The temperature was allowed to equilibrate for several minutes before taking each spectrum. Fluorescence spectra were collected systematically both with increasing and with decreasing temperature to understand the effects of photochemistry as well as temperature on the fluorescence intensities of samples that were initially highly-purified isomers. Emission spectra were corrected for the instrument response using a data file generated by a 200 W standard quartz tungsten-halogen filament lamp with spectral irradiance values traceable to NIST standards. For the display of spectra and the calculation of relative fluorescence yields, the emission spectra were converted to a wavenumber scale and intensities multiplied by λ^2 to give relative emission intensities in photons/s cm^{-1}.[30]

RESULTS AND DISCUSSION

Figure 1 shows the HPLC of the hexadecaheptaene sample before and after photoisomerization. One- and two-dimensional NMR spectroscopy (^{1}H-^{1}H COSY and ^{1}H-^{1}H NOESY) identify the peak eluting at ~8.5 min as the 4-*cis* isomer. This isomer dominates the products of the Wittig reaction, while the *all-trans* isomer is the major photochemical product. Irradiation of the pure *all-trans* isomer gives 4-*cis* hexadecaheptaene as the major photoproduct with the *all-trans* isomer dominating the photostationary state. The 4-*cis* and *all-trans* isomers thus are connected as major, but not exclusive photoisomerization products of each other. Extended irradiation indicates that, in addition to photoisomerization, there are a variety of other photochemical and thermal processes that lead to irreversible degradation of the samples.

Collection of the 4-*cis* and *all-trans* fractions from the HPLC allows the comparison of their room temperature absorption and emission spectra in pentadecane (Fig. 2). As noted in previous studies of a wide range of polyenes and carotenoids in solution,[31–33] the room temperature fluorescence spectra and fluorescence quantum yields of the *cis* and *trans* samples are very similar. Following S_0 ($1^1A_g^-$) → S_2 ($1^1B_u^+$) excitation, both isomers show dual emissions, S_2 ($1^1B_u^+$) → S_0 ($1^1A_g^-$) and S_1 ($2^1A_g^-$) → S_0 ($1^1A_g^-$), a signature of polyenes and carotenoids with intermediate conjugation lengths (N ≈ 6–8).[17,19,20,34,35] In *n*-pentadecane, the emission and absorption spectra of the heptaenes exhibit sufficient vibronic resolution to allow the identification of the (0–0) bands, providing an accurate measure of the energies of the S_1 ($2^1A_g^-$) and S_2 ($1^1B_u^+$) states of these isomers.

The 77 K fluorescence and fluorescence excitation spectra of 4-*cis* hexadecaheptaene in *n*-pentadecane are presented in Fig. 3. The high-resolution environment provided by the *n*-pentadecane matrix offer critical advantages in analyzing these spectra. The *n*-alkane mixed crystal selectively incorporates the polyene into a dominant substitutional site, providing well-defined, relatively homogeneous polyene-alkane interactions. This significantly decreases the inhomogeneous spectral broadening inherent to spectra obtained in solutions or low-temperature glasses. Although only the leading edge of the major 4-*cis* was collected from the HPLC (Fig. 1), the samples no doubt contain small amounts of other isomers. However, the high-resolution environments provided by the mixed crystals provide enhanced selectivity in exciting and detecting emission from the dominant 4-*cis* component in fluorescence emission

and excitation spectra. The use of *n*-alkane host crystals[36,37] has been exploited in several previous optical studies of simple polyenes,[18,27,38–40] including 2,4,6,8,10,12,14,16-octadecaoctaene, the longest linear polyene studied using low-temperature, high-resolution mixed-crystal techniques.[40]

The spectra of 4-*cis* hexadecaheptaene presented in Fig. 3 exhibit well-resolved vibronic progressions in the S_0 ($1^1A_g^-$) → S_2 ($1^1B_u^+$) absorption and the S_1 ($2^1A_g^-$) → S_0 ($1^1A_g^-$) emission. As noted in previous studies on model polyenes,[18,27,34,38–40] these progressions are dominated by combinations of totally symmetric carbon-carbon single and carbon-carbon double bond stretches built on easily identified electronic origins. The low temperature emission spectrum also shows features that can be identified with weak S_2 ($1^1B_u^+$) → S_0 ($1^1A_g^-$) fluorescence. In addition, the spectra allow the identification of relatively sharp vibronic bands due to the weak S_0 ($1^1A_g^-$) → S_1 ($2^1A_g^-$) transition on the low-energy tail of the strong S_0 ($1^1A_g^-$) → S_2 ($1^1B_u^+$) absorption. This transition is considerably more difficult to detect and identify in the much broader spectra of polyenes and carotenoids in room temperature solutions and low temperature glasses, illustrating another distinct benefit of the *n*-alkane matrices.

In contrast to the emission spectra obtained at room temperature, the 77 K fluorescence spectra (Fig. 4) of the 4-*cis* and *all-trans* isomers in *n*-pentadecane are remarkably different. The S_2 ($1^1B_u^+$) → S_0 ($1^1A_g^-$) emissions exhibit comparable intensities, with the *all-trans* isomer showing a small red shift in its somewhat better resolved spectrum (Fig. 4B). On the other hand, at 77 K the S_1 ("$2^1A_g^-$") → S_0 ("$1^1A_g^-$") emission of the 4-*cis* isomer is at least 20 times more intense than the S_1 ($2^1A_g^-$) → S_0 ($1^1A_g^-$) emission of the *trans* isomer (Fig. 4A). The dependence of the 4-*cis* emission yield on temperature is presented in Fig. 5. In order to compensate for fluctuations in fluorescence intensities in the flowing N_2 cryostat, we compare the ratio of integrated fluorescence intensities, $\varphi(S_1 \rightarrow S_0)/\varphi(S_2 \rightarrow S_0)$, for the two isomers. For the 4-*cis* isomer, the factor of ~15 change in this ratio is almost entirely due to the increase in S_1 ($2^1A_g^-$) → S_0 ($1^1A_g^-$) fluorescence upon cooling to 77 K. The corresponding ratio in the *all-trans* isomer shows a two-fold decrease when the sample is cooled. It is important to note that the weak S_1 ($2^1A_g^-$) → S_0 ($1^1A_g^-$) fluorescence observed for the *trans* isomer in part may be due to the photochemical production of highly fluorescent 4-*cis* and other *cis* impurities. The data indicated in Fig. 4 and 5 thus may underestimate the true difference between the low temperature S_1 (2^1A_g) → S_0 ($1^1A_g^-$) fluorescence yields of the pure 4-*cis* and pure *all-trans* isomers.

The *n*-alkane host offers a significant advantage for detecting the differences between S_1 ($2^1A_g^-$) → S_0 ($1^1A_g^-$) fluorescence yields in the two isomers at low temperature. The *n*-pentadecane mixed crystal preserves the planar, symmetric (C_{2h}) geometry of the *all-trans* heptaene, leading to relatively slow radiative decay for the symmetry-forbidden, S_1 ($2^1A_g^-$) → S_0 ($1^1A_g^-$) transition. Furthermore, the *n*-pentadecane environment provides sufficient optical resolution to differentiate between emissions due to the 4-*cis* and the *all-trans* species (Fig. 4). This is particularly important in distinguishing the weak emissions from the *trans* species from those of much more strongly emitting *cis* photochemical products. The differences between the fluorescence intensities of *cis* and *trans* samples are considerably less distinctive in the random environments provided by low temperature glasses (data not shown), which produce a distribution of distorted *trans* polyenes, many of which do not have C_{2h} symmetry.

The current work recalls a previous controversy regarding the origin of the fluorescence signals (*cis* impurities versus the dominant *trans* species) in samples of cold, isolated octatetraene, the most highly studied and best-understood linear polyene. Buma et al.[41] assigned the isolated molecule, S_0 ($1^1A_g^-$) → S_1 ($2^1A_g^-$) fluorescence excitation spectrum (obtained in a resonance-enhanced multiphoton ionization (REMPI) measurement) to a mono-*cis* isomer, arguing that

the *trans* species would have insufficient oscillator strength for fluorescence detection. A subsequent study by Petek, et al.,[42] on the high-resolution one- and two-photon fluorescence excitation spectra of octatetraene in supersonic jets, demonstrated that the oscillator strengths for the S_0 ($1^1A_g^-$) ↔ S_1 ($2^1A_g^-$) transitions in the *trans* isomer (induced by Herzberg-Teller vibronic coupling via low frequency b_u promoting modes) were comparable to the corresponding oscillator strengths for *cis* isomers. This results in fluorescence intensities from the *cis* and *trans* isomers of isolated octatetraene that mirror their ground state abundances, i.e., the fluorescence spectra can be identified with the dominant *trans* isomer in typical samples. The identification of *all-trans* octatetraene as the dominant emitting species was confirmed by analysis of the rotationally resolved S_0 ($1^1A_g^-$) → S_1 ($2^1A_g^-$) fluorescence excitation spectrum by Pfanstiel, et al.[43] These experiments established that the absorbing and emitting states both had *all-trans*, planar geometries and also demonstrated that the S_0 ($1^1A_g^-$) ↔ S_1 ($2^1A_g^-$) electronic transitions gain their intensities via vibronic coupling with the S_2 ($1^1B_u^+$) state.

The work presented here shows that, in contrast to octatetraene, the 4-*cis* isomer of hexadecaheptaene has a much higher $S_0 \leftrightarrow S_1$ oscillator strength than its *all-trans* counterpart. Under conditions where the *trans* isomer can be described by C_{2h} symmetry, e.g., in low-temperature *n*-pentadecane, the vibronically induced, S_1 ($2^1A_g^-$) → S_0 ($1^1A_g^-$) radiative decay is relatively slow, and the fluorescence can be dominated by heptaenes with distorted, s-*cis* or *cis* conformations, even though these species may be present in relatively low concentrations. The ability of *cis* isomers to dominate the fluorescence systematically increases with increasing conjugation length (manuscript in preparation).

The striking difference in temperature dependence of the fluorescence from the two isomers (Fig. 5) leads to the simple, qualitative model presented in Fig. 6. The thermodynamically favored *all-trans* isomer is connected to the 4-*cis* isomer by a relatively low energy barrier in the S_1 ($2^1A_g^-$) state. Our preliminary photochemical studies (Fig. 1) indicate that additional *cis* isomers also are accessible on the S_1 ($2^1A_g^-$) potential surface. Theoretical considerations also implicate s-*cis*, as well as distorted *trans* isomers on a complicated, multi-dimensional potential surface with many local minima, connected by relatively low barriers. However, since the 4-*cis* and *all-trans* isomers are the two major products of *all-trans* and 4-*cis* photoisomerization, we only consider these isomers in a much-simplified model (Fig. 6). The lower energy, *all-trans* isomer dominates the photostationary state, a common theme in polyene and carotenoid photochemistry.[44] Our model (Fig. 6) does not imply a mechanism for the isomerization; a detailed microscopic understanding of the chemistry would require additional experimental and theoretical work.

For the model presented in Figure 6, the S_1 ($2^1A_g^-$)→S_0 ($1^1A_g^-$) fluorescence quantum yield for the 4-*cis* isomer can be approximated by:

$$\varphi(T)=k_r/(k_r+k_{nr}+Ae^{-E_a/RT}) \quad (1)$$

We assume that the radiative and nonradiative decay rates are independent of temperature and that the 4-*cis* → *trans* isomerization proceeds over an activation barrier E_a. We also assume that the S_2 ($1^1B_u^+$)→S_0 ($1^1A_g^-$) fluorescence yield does not depend on temperature in fitting the data presented in Figure 5 to Equation 1. The resulting four-parameter fit (see Fig. 5) yields an activation energy of 4.3 ± 1.4 kcal and a pre-exponential factor (A) of 10^{10}–10^{12} s^{-1}. The fit is poorly determined, e.g., the parameters for the activation energy and pre-exponential factor are highly correlated with large uncertainties. The fits are heavily influenced by the high temperature data points, which include the melting of the *n*-pentadecane crystal at 10 °C. In addition to the least squares analysis, we also have employed simulations to explore the parameter space and to better understand the data and the model (Equation 1). The determination of relative fluorescence yields as a function of temperature on samples

undergoing photoisomerization is particularly challenging, especially for weakly emitting species. In spite of the limitations both of the model and the data, the parameters extracted from Equation 1 are consistent with thermally activated, 4-*cis* → *trans* isomerization in the S_1 state.

An identical model was postulated to account for the temperature dependence of S_1 lifetimes of *cis* and *trans* octatetraenes in different *n*-alkane solvents.[45] The temperature-dependences of the octatetraene S_1 lifetimes between 77 K and room temperature are comparable to the data presented in Fig. 5 and also were interpreted in terms of a thermally activated *cis* ⇆ *trans* isomerization in S_1 with pre-exponential factors of 10^{10}–10^{12} s^{-1} and activation energies of a few kcal/mol.[45,46] For example, analysis of lifetime data indicated an S_1 barrier of 1.1 kcal for the isomerization of *cis, trans*-1,3,5,7-octatetraene to the *all-trans* isomer[47] and 2.5 kcal for the reverse process.[45] The connections between the temperature dependence of the fluorescence lifetimes of octatetraene isomers and the fluorescent quantum yield data presented in Figure 5 with excited state isomerizations are buttressed by the temperature dependence of the photochemical quantum yields for *trans*→*cis* isomerizations in *all-trans* retinal. These studies indicate activation barriers of 1.6–3.2 kcal, depending on the solvent and the *cis* isomer formed.[48] It also is important to note that the barriers to C=C isomerization in the S_1 state are comparable to those for isomerization of carbon-carbon single bonds in polyene ground states.[46,49] This reflects the significant rearrangement of the C-C and C=C π-bond orders in going from the ground to the S_1 state.[50]

The low thermal barrier associated with the >20-fold increase in the S_1 ($2^1A_g^-$) → S_0 ($1^1A_g^-$) fluorescence intensity with decreasing temperature cannot be explained by isomerization on the ground state S_0 ($1^1A_g^-$) potential energy surface. It also is not consistent with isomerization in the short-lived S_2 state ($1^1B_u^+$). If that were the case, we would expect a substantial change with temperature in the quantum yield of S_2 ($1^1B_u^+$) → S_0 ($1^1A_g^-$) emission, which is not observed. The increase in the ratio, $\varphi(S_1 \rightarrow S_0)/\varphi(S_2 \rightarrow S_0)$, for the 4-*cis* isomer, thus is almost entirely due to the increase in S_1 ($2^1A_g^-$) → S_0 ($1^1A_g^-$) fluorescence upon cooling. Furthermore, in solutions, *trans* ↔ *cis* isomerization in S_1 ($2^1A_g^-$) must compete with rapid nonradiative processes, which tend to dominate the excited state decay of longer polyenes and carotenoids.[20]

The *all-trans* heptaene $S_1 \rightarrow S_0$ fluorescence yield shows a two-fold increase with temperature (Figure 5), suggesting that it crosses over a barrier in S_1 to a more fluorescent species. It is tempting to ascribe this weak emission as due to adiabatic conversion to 4-*cis* heptaene in our simple model. This would account for the rather similar room temperature fluorescence spectra of the *all-trans* and 4-*cis* species (Fig. 2) and the fact that the 4-*cis* isomer is the dominant photoisomerization product of *all-trans*-hexadecaheptaene. However, the very small fluorescence yields of the *all-trans* isomer at all temperatures make it difficult to identify its fluorescence with a particular asymmetric species. Adiabatic pathways to other *cis* isomers, distorted *trans* conformers, as well as isomerization upon relaxation to the ground state all could induce fluorescence in samples of pure, C_{2h}, *all-trans* hexadecaheptaene. It thus is much easier to make the case for *4-cis* → *all-trans* adiabatic S_1 conversion than for the reverse process.

The potential energy diagram presented in Fig. 6 is similar to that proposed by de Weerd et al.[51] based on subpicosecond dynamics studies of *all-trans* β-carotene. However, those authors suggested that β-carotene became distorted in the S_2 ($1^1B_u^+$) state and relaxed back to the *all-trans* configuration upon decaying to S_1 ($2^1A_g^-$). This is not the case for hexadecaheptaene, and other investigators have argued that conformational twisting occurs in S_1 ($2^1A_g^-$) in β-carotene[52] and other carotenoids.[52–54]

The relatively large oscillator strength for the S_0 ($1^1A_g^-$) ↔ S_1 ($2^1A_g^-$) transition in 4-*cis* hexadecaheptaene is confirmed by our ability to detect the S_0 ($1^1A_g^-$) → S_1 ($2^1A_g^-$) transition in the high-resolution fluorescence excitation spectrum (Fig. 7). The ~4700 cm^{-1} gap between the $1^1B_u^+$ and $2^1A_g^-$ states provides a wide window for observing the vibronic development of the $2^1A_g^-$ vibronic states built on the electronic origin (0-0) at 512 nm. Note also the coincidence between the 512 nm (0-0) bands in the S_0 ($1^1A_g^-$) → S_1 ($2^1A_g^-$) excitation spectrum (Fig. 7) and the S_1 ($2^1A_g^-$) → S_0 ($1^1A_g^-$) emission spectrum (Fig. 3). The overlap between electronic origins and the relatively strong $S_0 \rightarrow S_1$ absorption indicate a symmetry-allowed electronic transition, as expected for the 4-*cis* isomer. A large $S_0 \leftrightarrow S_1$ oscillator strength explains the considerable enhancement in the 4-*cis* $S_1 \rightarrow S_0$ fluorescence yield compared with that associated with the symmetry forbidden transition of the *all-trans* isomer. The excitation spectra for both the $S_0 \rightarrow S_1$ and $S_0 \rightarrow S_2$ absorptions show the classic pattern of vibronic intensities built on combinations of carbon-carbon single and double bond symmetric stretching modes. The vibronic spectrum shown in Fig. 7 previously was analyzed by Simpson et al. and assigned to the *all-trans* isomer.[18] However, our current work shows that the vibronic states observed are due to 4-*cis* hexadecaheptaene.

CONCLUSIONS

The results presented here require a reinterpretation of fluorescence experiments previously carried out on *all-trans* isomers of longer polyenes and of related carotenoids. Several previous studies of longer linear polyenes (N>4) have assigned $S_1 \rightarrow S_0$ fluorescence signals to *all-trans* isomers. Examples include the high-resolution work of Simpson et al. on hexadecaheptaene[18] and of Kohler et al. on octadecaoctaene.[40] The excitation and fluorescence spectra were assigned to *all-trans* species, but our work indicates that the $S_1 \rightarrow S_0$ emission spectra of these longer polyenes most likely are due to *cis* isomers, present as impurities or formed as photochemical products in the S_1 state. This is a significant finding, given that existing theoretical work (almost all on simple *all-trans* polyenes)[4,5,55,56] has been compared with experimental work on what now must be assigned to *cis* species. Rapid isomerization in S_1 ($2^1A_g^-$) explains the typically small differences between the S_1 ($2^1A_g^-$) → S_0 ($1^1A_g^-$) emission spectra and quantum yields of *cis* and *trans* systems in room temperature solutions. The almost negligible S_1 ($2^1A_g^-$) → S_0 ($1^1A_g^-$) fluorescence yields from C_{2h}, *trans* species and the relatively low resolution of solution and glass spectra prohibit a ready distinction between emissions due to *trans* isomers from those due to *cis* impurities or from *trans* molecules with conformational distortions that relax the rigorous selection rules. We thus conclude that, except for the very detailed studies of *all-trans* octatetraene, previous reports of S_1 emissions from *all-trans*, C_{2h} polyenes and carotenoids most likely are due to less symmetric species. These species may be present as ground state impurities, including photochemical products, or formed in the S_1 ($2^1A_g^-$) state following the excitation of *all-trans* polyenes.

Our results suggest that steady-state fluorescence experiments and time-resolved measurements, e.g., $S_1 \rightarrow S_N$ transient absorption experiments, detect different distributions of S_1 ($2^1A_g^-$) conformers and geometric isomers, even for samples with a single, *all-trans*, ground state structure. For example, the elegant S_1 ($2^1A_g^-$) → S_2 ($1^1B_u^+$) absorption experiments of Polívka et al.[57] on several *all-trans* carotenoids, including spheroidene, zeaxanthin and violaxanthin, were compared with the transition energies for the strongly allowed S_0 ($1^1A_g^-$) → S_2 ($1^1B_u^+$) absorptions. The energy difference in the electronic origins ((0–0) bands) of these two symmetry-allowed transitions yields the S_1 ($2^1A_g^-$) energy. However, S_1 electronic energies obtained in this manner were found to be consistently 500–1000 cm^{-1} lower than those from the fluorescence measurements. This is in accord with the model presented in Fig. 6. Fluorescence from these samples is from higher energy, distorted *trans* and/or *cis* carotenoids with $S_1 \leftrightarrow S_0$ oscillator strengths and radiative decay rates that

are sufficiently large to compete with the rapid (~10 ps) nonradiative decays in these molecules. It should be noted that Polívka et al.[58,59] suggested a similar model, though did not invoke isomerization, to explain the discrepancies between their results and the S_1 ($2^1A_g^-$) energies estimated by fluorescence techniques. Another conclusion from the current studies is that, at least for longer polyenes and related carotenoids, "forbidden" electronic transitions for molecules with C_{2h} symmetries will be very difficult to detect. Optical techniques that exploit the selection rules for allowed transitions, e.g., S_1 ($2^1A_g^-$) → S_2 ($1^1B_u^+$) absorption, thus have obvious advantages in accurately locating the excited electronic energy levels of *trans* polyenes and carotenoids.

The low energy barriers to isomerization and conformational distortion in S_1 ($2^1A_g^-$) are consistent with significant rearrangements of the ground state C-C and C=C bond orders relative to the changes in S_2 ($1^1B_u^+$) and other low-energy excited states.[3–5] This transposition of π-bond orders is a hallmark of polyene electronic structure and explains the unique ability of S_1 states to promote rapid isomerization. Low barriers to isomerization and conformational change also may account for the complex kinetics of S_2 ($1^1B_u^+$) → S_1 ($2^1A_g^-$) nonradiative decay in carotenoids. As mentioned previously, Cerullo, et al.[10] postulate the existence of an excited electronic state (S_x) between S_2 ($1^1B_u^+$) and S_1 ($2^1A_g^-$) that decays on a ~ 100 fs time scale, and van Grondelle et al.[11] hypothesize that additional short-lived electronic singlet states (S* and $S^‡$) provide alternate routes for internal conversion from S_2. The current work strongly suggests that at least some of these proposed singlet electronic states instead may be manifestations of nonradiative decay on complicated S_1 ($2^1A_g^-$) potential surfaces. These surfaces provide multiple pathways for the zero-point level of S_2 ($1^1B_u^+$) to change its geometry to arrive at vibrationally relaxed, thermally equilibrated S_1 ($2^1A_g^-$).

Supplementary Material

Refer to Web version on PubMed Central for supplementary material.

Acknowledgements

We thank Tomáš Polívka and Robert Birge for fruitful discussions. RLC has been supported by the Bowdoin College Kenan and Porter Fellowship Programs and acknowledges funding from NSF-ROA (MCB-0314380 to HAF) and the Petroleum Research Fund, administered by the American Chemical Society. RLC also was supported in this work while serving at the National Science Foundation. This research is supported in the laboratory of HAF by the National Institutes of Health (GM-30353) and the University of Connecticut Research Foundation. HH and RF acknowledge grants-in-aid (# 17204026 and 17654083) from the Japanese Ministry of Education, Culture, Sports, Science and Technology. HH and RF also acknowledge financial support from the Strategic International Cooperative Program of the Japan Science and Technology Agency. We also acknowledge the helpful comments of one of the referees in clarifying our understanding of the role of adiabatic photoisomerization in hexadecaheptaene.

References

1. Hudson B, Kohler B. Ann Rev Phys Chem 1974;25:437–460.
2. Hudson, BS.; Kohler, BE.; Schulten, K. Linear polyene electronic structure and potential surfaces. In: Lim, ED., editor. Excited States. 6. Academic Press; New York: 1982. p. 1-95.
3. Schulten K, Karplus M. Chem Phys Lett 1972;14:305–309.
4. Tavan P, Schulten K. J Chem Phys 1986;85:6602–6609.
5. Tavan P, Schulten K. Phys Rev B: Condens Matter 1987;36:4337–4358. [PubMed: 9943414]
6. Sashima T, Koyama Y, Yamada T, Hashimoto H. J Phys Chem B 2000;104:5011–5019.
7. Fujii R, Onaka K, Nagae H, Koyama Y, Watanabe Y. J Luminescence 2001;92:213–222.
8. Zhang JP, Inaba T, Watanabe Y, Koyama Y. Chem Phys Lett 2000;332:351–358.
9. Koyama Y, Rondonuwu FS, Fujii R, Watanabe Y. Biopolymers 2004;74:2–18. [PubMed: 15137086]
10. Cerullo G, Polli D, Lanzani G, De Silvestri S, Hashimoto H, Cogdell RJ. Science 2002;298:2395–2398. [PubMed: 12493917]

11. Gradinaru CC, Kennis JTM, Papagiannakis E, van Stokkum IHM, Cogdell RJ, Fleming GR, Niederman RA, van Grondelle R. Proc Natl Acad Sci USA 2001;98:2364–2369. [PubMed: 11226245]
12. Larsen DS, Papagiannakis E, van Stokkum IHM, Vengris M, Kennis JTM, van Grondelle R. Chem Phys Lett 2003;381:733–742.
13. Kukura P, McCamant DW, Mathies RA. J Phys Chem A 2004:108.
14. Kosumi D, Komukai M, Hashimoto H, Yoshizawa M. Phys Rev Lett 2005;95:213601–213604. [PubMed: 16384139]
15. Kohler BE, Terpougov V. J Chem Phys 1998;108:9586–9593.
16. Christensen RL, Kohler BE. J Phys Chem 1976;80:2197–2200.
17. Christensen RL, Barney EA, Broene RD, Galinato MGI, Frank HA. Arch Biochem Biophys 2004;430:30–36. [PubMed: 15325909]
18. Simpson JH, McLaughlin L, Smith DS, Christensen RL. J Chem Phys 1987;87:3360–3365.
19. Snyder R, Arvidson E, Foote C, Harrigan L, Christensen RL. J Am Chem Soc 1985;107:4117–4122.
20. Frank HA, Josue JS, Bautista JA, van der Hoef I, Jansen FJ, Lugtenburg J, Wiederrecht G, Christensen RL. J Phys Chem B 2002;106:2083–2092.
21. Shima S, Ilagan RP, Gillespie N, Sommer BJ, Hiller RG, Sharples FP, Frank HA, Birge RR. J Phys Chem A 2003;107:8052–8066.
22. Fujii R, Onaka K, Kuki M, Koyama Y, Watanabe Y. Chem Phys Lett 1998;288:847–853.
23. Josue JS, Frank HA. J Phys Chem A 2002;106:4815–4824.
24. Frank HA, Bautista JA, Josue JS, Young AJ. Biochemistry 2000;39:2831–2837. [PubMed: 10715102]
25. Onaka K, Fujii R, Nagae H, Kuki M, Koyama Y, Watanabe Y. Chem Phys Lett 1999;315:75–81.
26. Andersson PO, Bachilo SM, Chen RL, Gillbro T. J Phys Chem 1995;99:16199–16209.
27. Auerbach RA, Christensen RL, Granville MF, Kohler BE. J Chem Phys 1981;74:4–9.
28. D'Amico KL, Manos C, Christensen RL. J Am Chem Soc 1980;102:1777–1782.
29. Palmer B, Jumper B, Hagan W, Baum JC, Christensen RL. J Am Chem Soc 1982;104:6907–6913.
30. Lakowicz, JR. Principles of Fluorescence Spectroscopy. 2. Kluwer Academic, Plenum Publishers; New York: 1999.
31. Bautista JA, Chynwat V, Cua A, Jansen FJ, Lugtenburg J, Gosztola D, Wasielewski MR, Frank HA. Photosyn Res 1998;55:49–65.
32. Andersson PA, Takaichi S, Cogdell RJ, Gillbro T. Photochem Photobiol 2001;74:549–557. [PubMed: 11683034]
33. Frank HA, Desamero RZB, Chynwat V, Gebhard R, van der Hoef I, Jansen FJ, Lugtenburg J, Gosztola D, Wasielewski MR. J Phys Chem A 1997;101:149–157.
34. Christensen, RL. The electronic states of carotenoids. In: Frank, HA.; Young, AJ.; Britton, G.; Cogdell, RJ., editors. The Photochemistry of Carotenoids. 8. Kluwer Academic Publishers; Dordrecht: 1999. p. 137-159.
35. DeCoster B, Christensen RL, Gebhard R, Lugtenburg J, Farhoosh R, Frank HA. Biochim Biophys Acta 1992;1102:107–114. [PubMed: 1510992]
36. Shpol'skii EV. Sov Phys Usp 1962;5:522–531.
37. Shpol'skii EV. Sov Phys Usp 1963;6:411–427.
38. Christensen RL, Kohler BE. J Chem Phys 1975;63:1837–1846.
39. Andrews JR, Hudson BS. J Chem Phys 1978;68:4587–4594.
40. Kohler BE, Spangler C, Westerfield C. J Chem Phys 1988;89:5422–5428.
41. Buma WJ, Kohler BE, Shaler TA. J Chem Phys 1992;96:399–407.
42. Petek H, Bell AJ, Choi YS, Yoshihara K, Tounge BA, Christensen RL. J Chem Phys 1993;98:3777–3794.
43. Pfanstiel JF, Pratt DW, Tounge BA, Christensen RL. J Phys Chem A 1999;103:2337–2347.
44. Zechmeister, L. Cis-trans isomeric carotenoids, vitamin A, and arylpolyenes. Academic Press; New York: 1962.
45. Kohler BE, Mitra P, West P. J Chem Phys 1986;85:4436–4440.

46. Kohler BE. Chem Rev 1993;93:41–54.
47. Ackerman JR, Kohler BE. J Am Chem Soc 1984;106:3681–3682.
48. Waddell WH, Chihara K. J Am Chem Soc 1981;103:7389–7390.
49. Ackerman JR, Kohler BE. J Chem Phys 1984;80:45–50.
50. Schulten K, Ohmine I, Karplus M. J Chem Phys 1976;64:4422–4441.
51. de Weerd FL, van Stokkum IHM, van Grondelle R. Chem Phys Lett 2002;354:38–43.
52. Kosumi D, Yanagi K, Nishio T, Hashimoto HMY. Chem Phys Lett 2005;408:89–95.
53. Billsten HH, Pan J, Sinha S, Pascher T, Sundström V, Polívka T. J Phys Chem A 2005;109:6852–6859. [PubMed: 16834041]
54. Pendon ZD, Gibson GN, van der Hoef I, Lugtenburg J, Frank HA. J Phys Chem B 2005;109:21172–21179. [PubMed: 16853743]
55. Tavan P, Schulten K. J Chem Phys 1979;70:5407–5413.
56. Head-Gordon M, Rico RJ, Oumi M, Lee TJ. Chem Phys Lett 1994;219:21–29.
57. Polívka T, Herek JL, Zigmantas D, Akerlund HE, Sundström V. Proc Nat Acad Sci USA 1999;96:4914–4917. [PubMed: 10220393]
58. Polívka T, Zigmantas D, Frank HA, Bautista JA, Herek JL, Koyama Y, Fujii R, Sundström V. J Phys Chem B 2001;105:1072–1080.
59. Polívka T, Sundström V. Chem Rev 2004;104:2021–2071. [PubMed: 15080720]

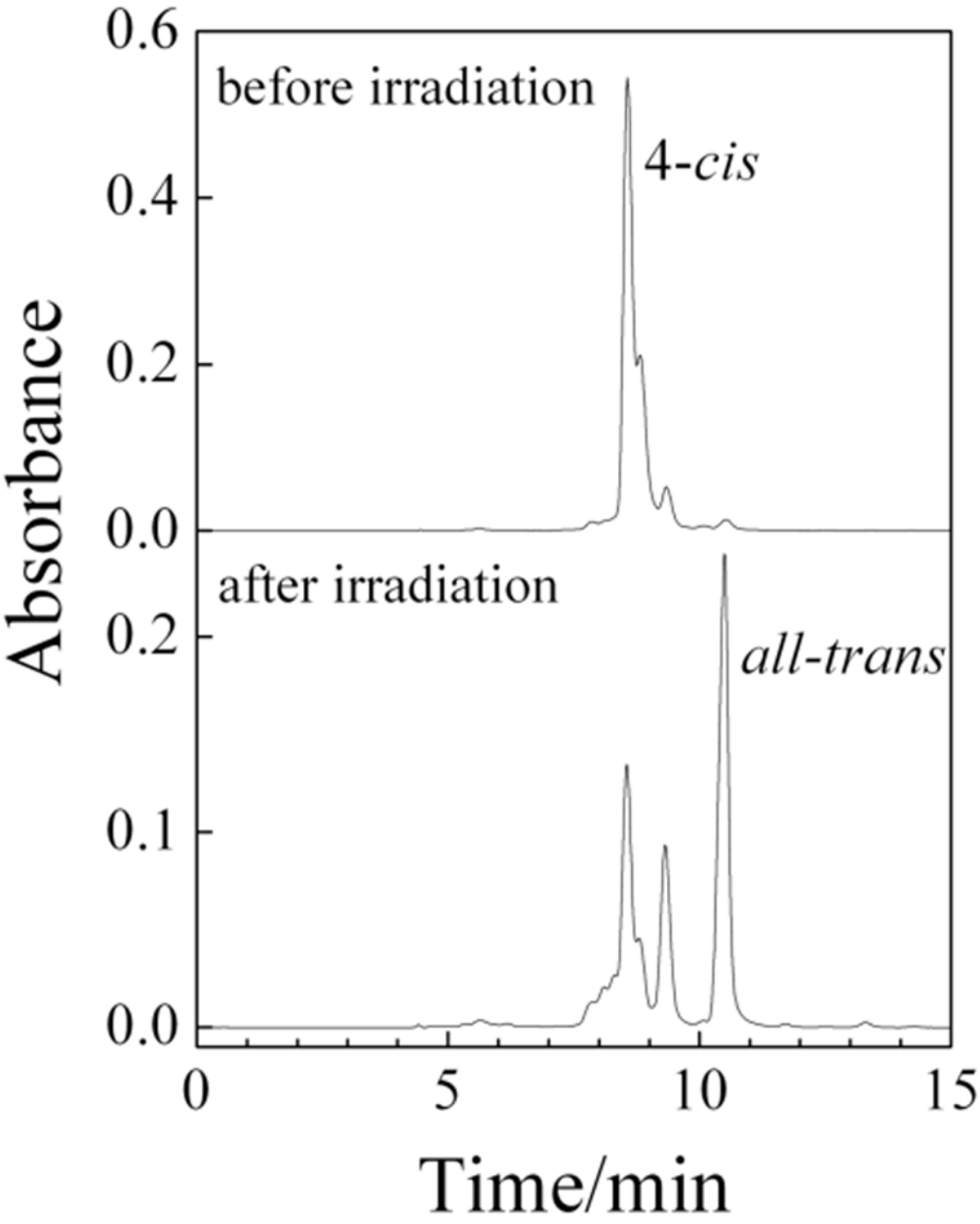

Figure 1.
HPLC of hexadecaheptaene before and after 396 nm irradiation. Chromatography was done on a C_{18} reverse phase column using acetonitrile as the mobile phase. Absorbance was monitored at 396 nm.

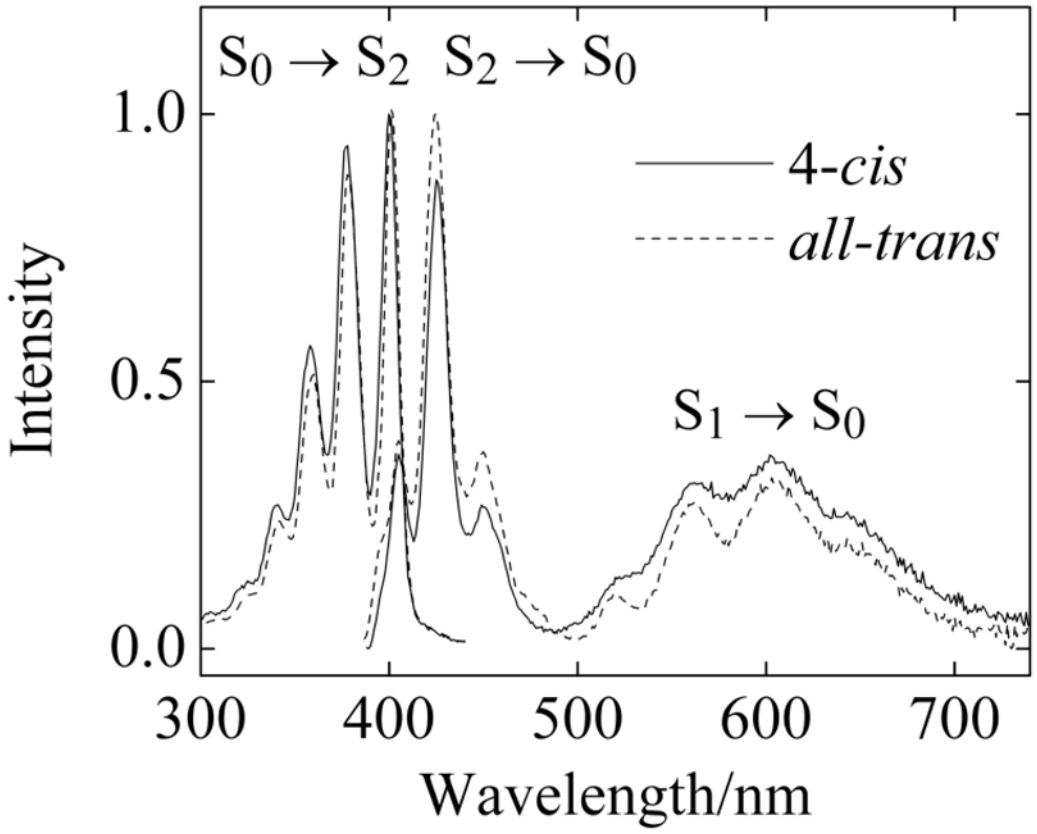

Figure 2.
Absorption and fluorescence spectra of 4-*cis* (378 nm excitation) and *all-trans* (377 nm excitation) hexadecaheptaene in *n*-pentadecane at room temperature. The absorption spectra are normalized to their maximum values. Maximum absorbances of ~0.10 minimized the effects of self-absorption. The fluorescence intensities have been corrected for the different room temperature absorbances of the two samples at the excitation wavelengths. Spectra were acquired with 1-nm bandpasses.

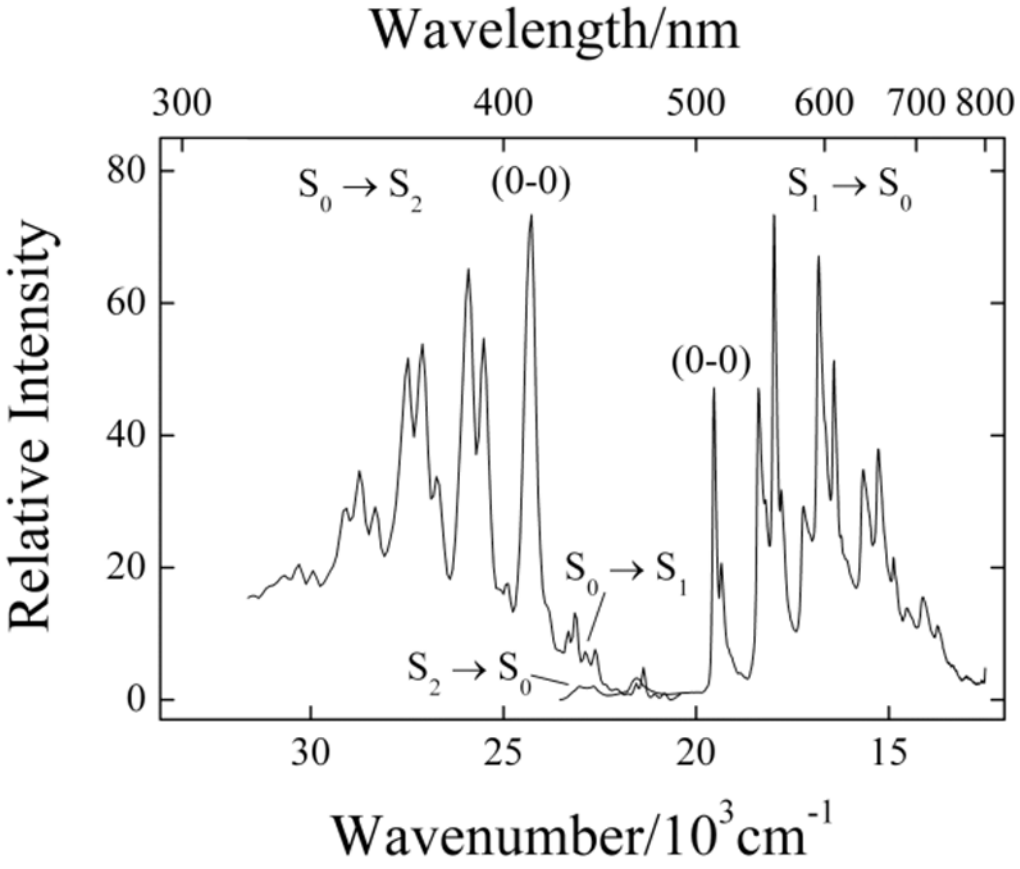

Figure 3.

Fluorescence excitation and emission spectra of 4-*cis* hexadecaheptaene in *n*- pentadecane at 77 K. The fluorescence spectrum was obtained by exciting at 411 nm, and the fluorescence excitation spectrum was monitored at 594 nm. Maximum absorbances of ~0.10 minimized the effects of self-absorption. Fluorescence intensities were corrected for the different room temperature absorbances of the two samples at the excitation wavelengths. Spectra were acquired with 1-nm bandpasses.

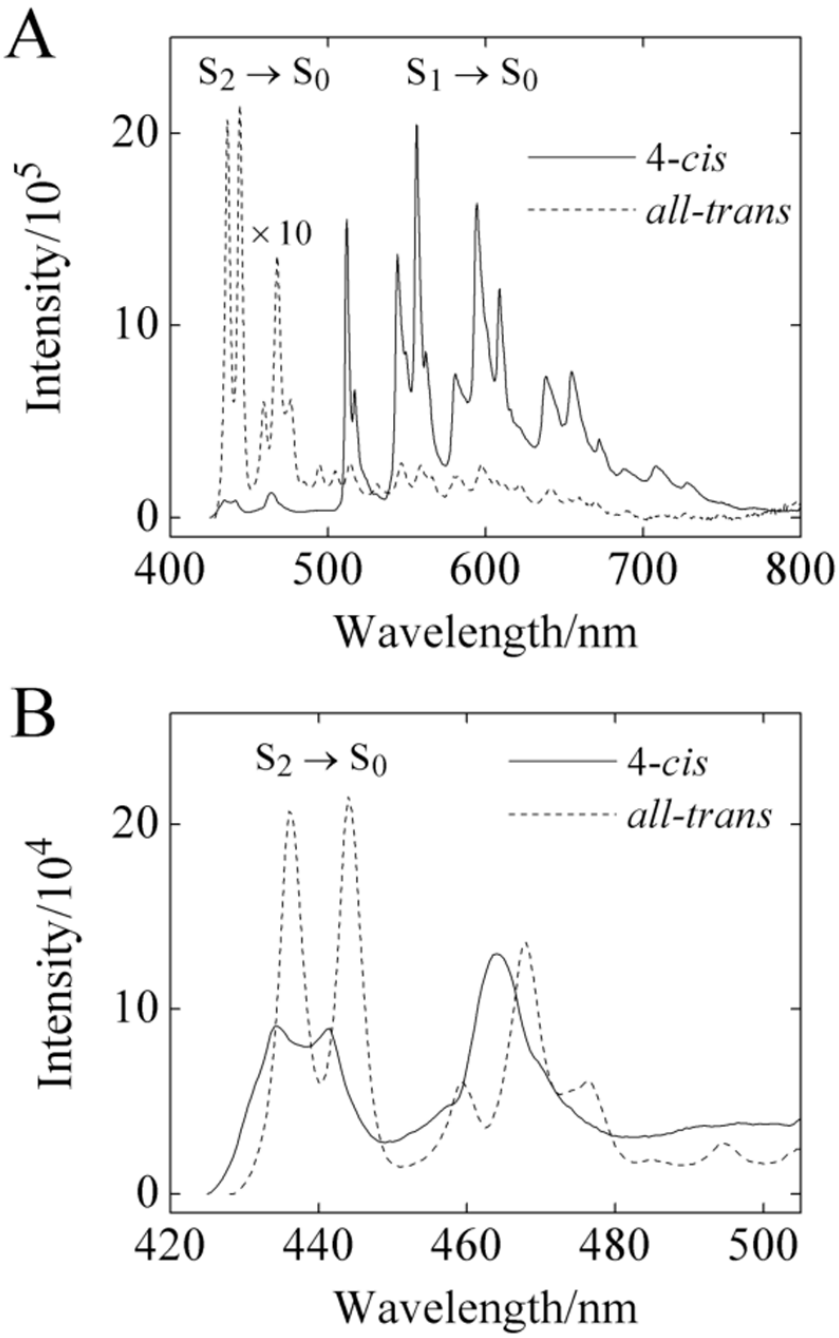

Figure 4.

A) Comparison of fluorescence spectra of 4-*cis* and *all-trans* hexadecaheptaene in *n*-pentadecane at 77 K. The relative fluorescence intensities have been corrected for the difference in the room temperature absorbances of the two samples. Emission spectra were obtained by exciting into the $S_0 \rightarrow S_2$ (0–0) bands (414 nm for *all-trans*, 411 nm for 4-*cis*). B) Expanded view of (A) showing the $S_2 \rightarrow S_0$ fluorescence spectra of 4-*cis* hexadecaheptaene and *all-trans* hexadecaheptaene in *n*-pentadecane at 77 K. Emission bandpasses were 1 nm for all spectra.

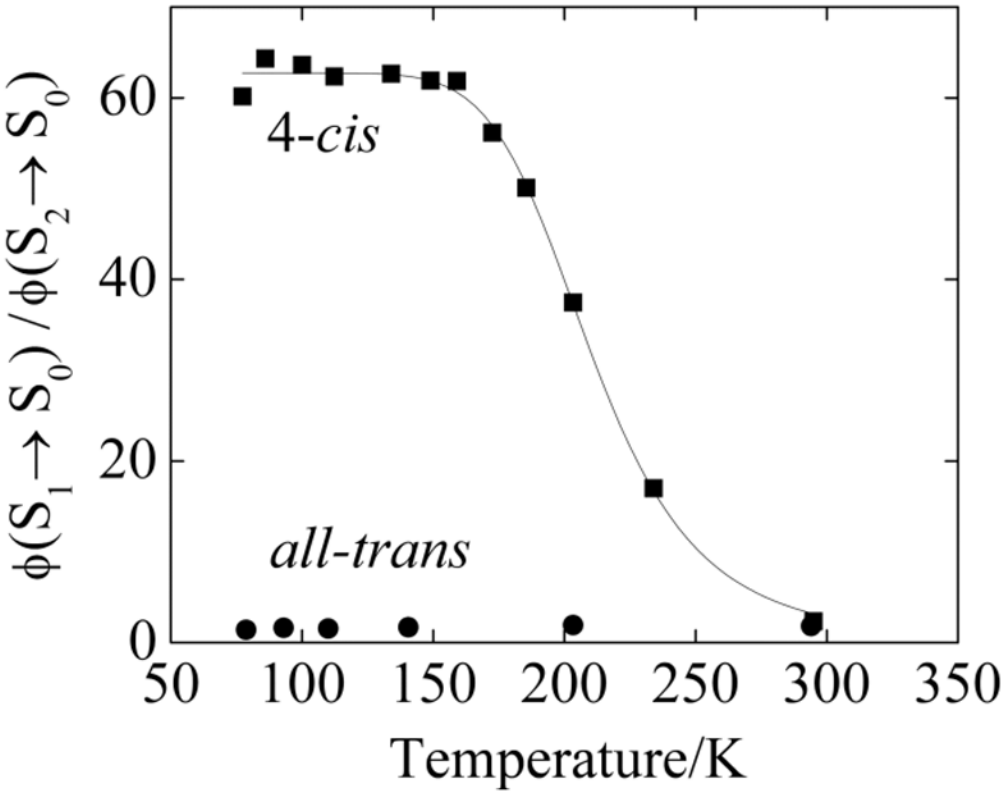

Figure 5.

Ratios of integrated fluorescence yields ($\varphi(S_1 \rightarrow S_0)/\varphi(S_2 \rightarrow S_0)$) for 4-*cis*- (squares) and *all-trans* (circles) hexadecaheptaene as a function of temperature. The temperature dependence of the ratio for the 4-*cis* isomer was fit to Equation 1 assuming that k_r, k_{nr}, and $\varphi(S_2 \rightarrow S_0)$ are independent of temperature. The four-parameter fit (solid line) gives $E_a = 4.3 \pm 1.4$ kcal.

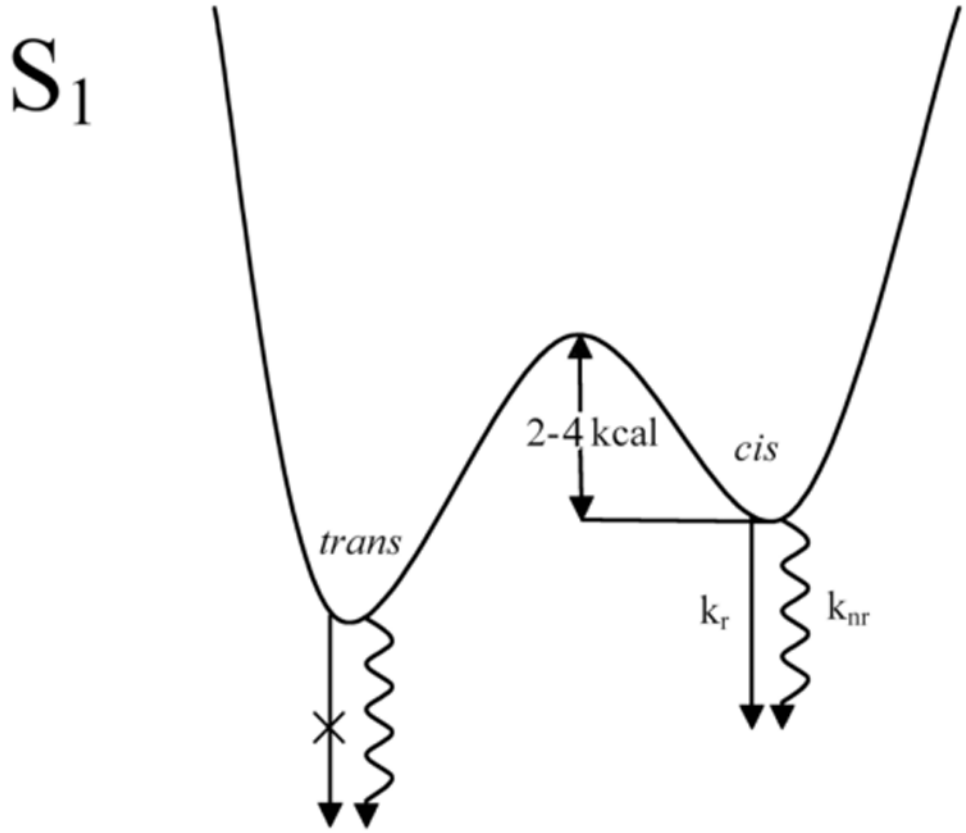

Figure 6.
Schematic potential energy surface for hexadecaheptaene in the S_1 ($2^1A_g^-$) state.

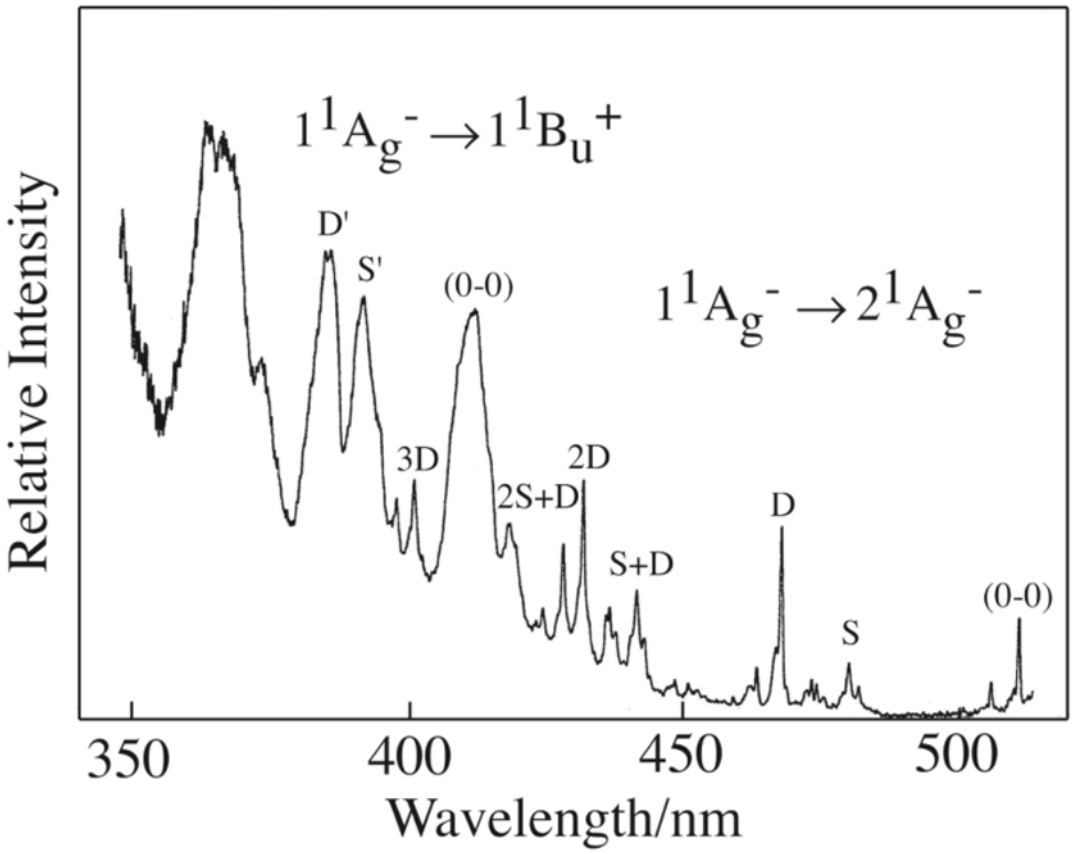

Figure 7.

Fluorescence excitation spectra ($1^1A_g^- \rightarrow 2^1A_g^-$ and $1^1A_g^- \rightarrow 1^1B_u^+$) of 4-*cis*-2,4,6,8,10,12,14-hexadecaheptaene in 10 K *n*-pentadecane. Fluorescence was detected at 560 nm. Vibronic features labeled with S and D (and S′ and D′) indicate combinations of C-C and C=C symmetric stretching modes. This spectrum was obtained on a more concentrated sample than that used for the excitation spectrum presented in Fig. 3. This amplifies the $1^1A_g^- \rightarrow 2^1A_g^-$ absorption. The excitation spectrum is not corrected for the wavelength dependence of the excitation system. (Figure adapted by the author, RLC, from Figure 3 of Reference 18).